Deep-Sea Research II 123 (2016) 30–41

Contents lists available at ScienceDirect

Deep-Sea Research II

journal homepage: www.elsevier.com/locate/dsr2

Taxonomic variability of phytoplankton and relationship with production of CDOM in the polynya of the Amundsen Sea, Antarctica

Yoon Chang Lee [a], Mi Ok Park [a,*], Jinyoung Jung [b], Eun Jin Yang [b], Sang Hoon Lee [b]

[a] Pukyong National university, 45 Yong-so Street, Yongso-ro, Namgu, Busan 608-737, South Korea
[b] Korea Polar Research Institute, Songdomirae-ro, Yeonsugu, Incheon 406-840, South Korea

ARTICLE INFO

Available online 30 September 2015

Keywords:
Chl-a
CDOM
Diatoms
Phaeocystis
Polynya
The Amundsen Sea

ABSTRACT

To evaluate the relationship between the phytoplankton composition and the CDOM production in the Amundsen Sea, we examined the taxonomic variability of phytoplankton, nutrients and chromophoric dissolved organic matter (CDOM) participating in two research cruises, ANA02C (February, 2012) and ANA04B (January, 2014). For both cruises, the peak concentrations of chlorophyll a (Chl-a) were measured in the Amundsen Sea Polynya (ASP) where the average Chl-a concentration was 2.31 $\mu g\ L^{-1}$ ($\pm$ 1.01 $\mu g\ L^{-1}$) in February 2012 and 3.92 $\mu g\ L^{-1}$ ($\pm$ 3.14 $\mu g\ L^{-1}$) in January 2014. The major phytoplankton groups were diatoms and prymnesiophytes, while the minor groups were cryptophytes, chlorophytes, dinophytes, chrysophytes and cyanophytes. The phytoplankton compositions in the sea ice zone (SIZ), the ASP and ice shelf (IS) was distinct. The predominance of *Phaeocystis antarctica* (*P. antarctica*) (70–90%) was observed at all stations, except in the SIZ in January 2014. While the CDOM concentrations (a_{355}) ranged from 0.07 to 0.98 m^{-1}, the average values of a_{355} of the euphotic layer in the ASP was 0.51 m^{-1} ($\pm$ 0.19 m^{-1}), which was much higher than any other region of the Southern Ocean. CDOM showed strong correlation with Chl-a but no relationship with salinity, which implies that biological processes were the main source of CDOM. Among the major phytoplankton taxa, *P. antarctica* was confirmed as the most important contributor to the production of CDOM, according to the high correlation between marker pigment (hex-fuco) and CDOM. The unusually high CDOM in the ASP is expected to give as impact on the environment in various aspects. As a nature of CDOM, absorption of solar radiation at the surface can result in the increase of sea surface temperature (SSTs), which will accelerate the ice melting. Also the photo-oxidation of CDOM can serve as a feedback to increasing atmospheric CO_2 concentrations after peak bloom in austral summer.

1. Introduction

While the Southern Ocean is characterized by high nutrients and low chlorophyll (HNLC) with a relatively deep mixed layer and low amounts of trace metals such as iron (Fe), the polynyas around Antarctica show exceptionally high productivity (Arrigo et al., 2008; Arrigo and van Dijken, 2003). In particular, the Amundsen Sea Polynya (ASP) shows the highest primary production among 37 identified coastal polynyas in the Southern Ocean (Arrigo and van Dijken, 2003). Since the Southern Ocean plays an important role in the global carbon cycle, accounting for 20% of global ocean CO_2 uptake (Takahashi et al., 2009), variation in phytoplankton taxa and primary production in the highly productive polynyas can profoundly influence the marine carbon cycle including carbon export and production of CDOM in the Southern Ocean.

The air-sea carbon fluxes of seasonally ice-covered ocean is sensitive to changes in the timing of seasonal sea ice, because of the balance between the potential for ventilation of CO_2-rich waters in late winter/early spring versus CO_2 drawdown by high rate of biological production in spring/summer (Yager et al., 1995). Sea ice coverage decreased in the Bellingshausen-Amundsen Seas from 1979 to 2006 and the melting rate of ice shelves has been accelerated recently (Fragoso and Smith, 2012; Rignot, 2001). This trend is predicted to continue into the future. Climate changes in the Antarctica are playing increasingly significant role in regulating the size of the carbon sink in the Southern Ocean. There is no doubt that Antarctic polynyas are highly climate-sensitive, undergoing radical change like the ASP and Mertz Glacial Polynya (Shadwick et al., 2013).

* Corresponding author. Tel.: +82 51 629 6575.
E-mail address: mokpark@pknu.ac.kr (M.O. Park).

http://dx.doi.org/10.1016/j.dsr2.2015.09.002
0967-0645/

CDOM is the optically active component of DOM (Barbini et al., 2003; Nelson and Siegel, 2002), which absorbs light at ultraviolet (UV) and visible wavelengths (Hansell and Carlson, 2002; Kieber et al., 1989). CDOM regulates the color of the ocean, light penetration, and photochemical reactions that influence the carbon cycle (Bricaud et al., 1981; Zepp et al., 2007). In addition, the presence of CDOM affects biogeochemistry and biology of the Southern Ocean through radiative heating (Pegau, 2002; Hill, 2008) and the photoprotection of marine organisms from UV light (Norman et al., 2011; Osburn et al., 2009).

Since the production of CDOM is known to have a multiple paths (such as microorganism degradation, metabolic byproducts of phytoplankton, and photolysis of DOM), it is very complicated to find the main factors that control the production of CDOM in marine environment. However, the majority of organic carbon in the open ocean is known to be produced photosynthetically by phytoplankton. Recently, Ortega-Retuerta et al. (2010) described the geographical and vertical distribution of CDOM in the Antarctic Peninsula area and reported a positive correlation between CDOM and both Chl-a and bacterial production in the Weddell Sea. This suggests that phytoplankton is one of the major sources of CDOM (Carlson and Ducklow, 1996).

At the beginning period of CDOM research, CDOM was considered as a refractory pool formed by slow-cycling compounds. The active research started very recently only after the recognition of short residence time and contemporary origin of CDOM (Amon and Benner, 1994). Ortega-Retuerta et al. (2010) reported the highly photoreactive nature of CDOM, with half lives ranging from 2.1 to 5.1 days due to photobleaching in the upper layer and also photohumification in the Antarctic Peninsula.

Because of the highest primary productivity observed in the ASP among the 28 polynyas in Southern Ocean, export efficiency during peak bloom conditions in the ASP is expected high. In fact, the ASPIRE expedition investigated the particle flux (sediment trap), zooplankton fecal pellets, and bacterial respiration during austral summers of 2010 and 2011. The total annual capture of particle flux was 315 mmol C/m^2 which exceeded the comparable WAP observation (Ducklow et al., 2015). Also they reported that pCO_2 in the central part of the ASP was highly underestimated as low as 100 ppm, which is nearly 300 ppm below atmospheric concentration. Overall, the ASP is regarded as a fairly efficient export system for carbon sequestration. However, most of the sinking particles are decomposed and remineralized between the bottom of euphotic zone and ~1000 m (Martin et al., 1987). And the decomposed particulate organic matter (POM) contributes to the DOM pool including CDOM in the water column. In turn, the increased CDOM can be either remineralized by photobleaching under the solar radiation during summer or absorb the heat energy at the surface. So CDOM is one of the missing factors which should be considered, for better understanding the efficiency of export of POM related with carbon cycles in this climate-sensitive ecosystem and the acceleration of ice melting in the ASP. In other words, if we want to find the fate of sinking particles in the ASP which might result in the increase the atmospheric CO_2 concentration by microbial process and photobleaching, it is necessary to know the major source and photoreactivity of CDOM.

The ASP is located in one of the most rapidly and profoundly changing regions in the Southern Ocean. We lack even a qualitative understanding of how the ASP ecosystem will respond to continued sea ice loss and the possible collapse of the West Antarctic ice shelves. Thus, in order to understand the relationship between phytoplankton community structure and CDOM production in the Amundsen Sea, we investigated the distribution and properties of CDOM, phytoplankton taxonomy and related environmental factors in our study area during two Amundsen Sea cruises conducted in austral summer of 2012 and 2014.

2. Materials and methods

2.1. Study area

Based on sea ice distribution and concentration data, the study area was divided into three regions: the sea ice zone (SIZ), the Amundsen Sea Polynya (ASP), and the ice shelf (IS). The first cruise, ANA02C, was conducted from January 31 to March 20, 2012 onboard the Korean icebreaker research vessel (IBRV), Araon. Water samples and environmental data were collected in the Amundsen Sea (Table 1). A polynya is defined as an area of open water within the SIZ (Arrigo and van Dijken, 2003). Sea ice concentration data were obtained from the Advanced Microwave Scanning Radiometer-Earth Observing System (AMSR-E) sensor on the National Aeronautics and Space Administration (NASA) Aqua Satellite and also from the National Snow and Ice Date Center. Sampling locations of ANA02C cruise are shown in Fig. 1a. CTD casts were conducted at 52 stations during first cruise. In addition, 15 stations were selected for high-performance liquid chromatography (HPLC) analysis of photosynthetic pigments.

The second cruise was also conducted onboard the IBRV Araon in the Amundsen Sea from December 24, 2013 to January 16, 2014 (Fig. 1b). CTD casts were conducted at 32 stations during the second cruise; 15 stations were selected for HPLC analysis and 8 stations were selected for CDOM analysis (Table 1).

2.2. Pigment analysis by HPLC

For each station, pigment analysis samples for phytoplankton were collected from the surface to the 100 m depth. 1.5 L of seawater was filtered through 47 mm GF/F filters. The filters were then frozen in liquid nitrogen, transported to the lab and stored at −80 °C until subsequent analysis. The analysis procedures and calibration method were previously reported by Park and Park (1997).

Chlorophyll a (Chl-a), Chlorophyll b (Chl-b), chlorophyll c_2 (Chl-c_2), chlorophyll c_3 (Chl-c_3), 19′-hexanoyloxyfucoxanthin (hex-fuco), fucoxanthin (fuco), 19′-butanoyloxyfucoxanthin (but-fuco) alloxanthin (allo), peridinin (perid), violaxanthin (viola), zeaxanthin (zea), lutein (lut), diadinoxanthin (DD), and diatoxanthin (DT) were measured to used as proxies for estimating relative proportions of phytoplankton group taxa. The biomarkers for chlorophytes, prymnesiophytes, diatoms, chrysophytes, cryptophytes, dinophytes and cyanophytes are chl b, hex-fuco, fuco, but-fuco, allo, perid and zea. The concentrations of standard pigments were calibrated by spectrophotometry with the known specific extinction coefficients from Jeffrey et al. (1997). The absorbance was measured at maximum absorbance and minimum absorbance (750 nm). The equation for pigment concentration was explained by Park (1999).

$$C\left(\mu g L^{-1}\right) = \frac{\text{absorbance}}{\varepsilon\left(\text{Lg}^{-1}\text{cm}^{-1}\right) \times (\text{cm})} \times \frac{10^6\ \mu g}{g}$$

C: concentration of pigment, ε: extinction coefficient

2.3. Phytoplankton taxonomic composition

Spatial distributions of the major phytoplankton taxa in the Amundsen Sea were inferred from HPLC analysis of phytoplankton pigments. Marker pigments were used to distinguish the major taxa: hex-fuco for *Phaeocystis* spp., fuco for diatoms, and allo for cryptophytes. The accessory pigment:Chl-a ratios facilitated the comparison of the dominance of a particular phytoplankton class with respect to the total phytoplankton community. Among pigment:Chl-a ratios, we used hex-fuco:Chl-a and fuco:Chl-a ratios

Table 1
Locations of sampling stations during austral summer in the Amundsen Sea in 2012 and 2014.

ANA02C (February, 2012)

Station	Depth(m)	Work	Sampling depth(m)						
1	469	Chl a, Pigments	0	10	20	30	50	70	100
2	539	Chl a, Pigments	0	10	20	30	50	70	100
3	608	Chl a, Pigments	0	10	20	30	50	70	100
85	1499	Chl a, Pigments	0	10	20	30	50	70	100
8	364	Chl a, Pigments	0	10	20	30	50	70	100
10	810	Chl a, Pigments	0	10	20	30	50	70	100
12	498	Chl a, Pigments	0	10	20	30	50	70	100
16	520	Chl a, Pigments	0	10	20	30	50	70	100
17	712	Chl a, Pigments	0	10	20	30	50	70	100
71	624	Chl a, Pigments	0	10	20	30	50	70	100
17-1	709	Chl a, Pigments	0	10	20	30	50	70	100
19	1063	Chl a, Pigments	0	10	20	30	50	70	100
22	1031	Chl a, Pigments	0	10	20	30	50	70	100
24	1055	Chl a, Pigments	0	10	20	30	50	70	100
27	989	Chl a, Pigments	0	10	20	30	50	70	100

ANA04B (January, 2014)

Station	Depth(m)	Euphotic depth (m)	Work	Sampling depth(m)												
1	3491	40	CDOM, Chl.a, Pigment, Nutrients	0*	20*	30*	40	60*	75	100*	750*	1000*	1500*			
2	3249	43	CDOM, Chl.a, Pigment, Nutrients	0*	20	40*	60	75	100*	300*	500*	1000*	1500*	2000*		
3	611	18	Chl.a, Pigment, Nutrients	0	10	25	40	60	100							
4	509	13	CDOM, Chl.a, Pigment, Nutrients	0*	10	20*	40	50*	60	100*	300*	450*	508*			
5	528	15	Chl.a, Pigment, Nutrients	0	10	25	40	60	100							
10	590	11	CDOM, Chl.a, Pigment, Nutrients	0*	15*	25	40*	60	80*	100*	120*	200*	350*	500*	590*	
13	712	10	Chl.a, Pigment, Nutrients	0	10	20	40	60	100							
14	821	11	CDOM, Chl.a, Pigment, Nutrients	0*	10	20*	40	60*	80*	100*	150*	240*	330*	590*	630*	820*
19	704	12	CDOM, Chl.a, Pigment, Nutrients	0*	15	20*	40*	60	80*	100*	160*	300*	703*			
22	624	20	Chl.a, Pigment, Nutrients	0	10	20	40	60	100							
24	1040	17	CDOM, Chl.a, Pigment, Nutrients	0*	10	20*	40	60*	100*	120*	350*	500*	660*	850*	1040*	
26	670	13	Chl.a, Pigment, Nutrients	0	10	20	40	60	100							
27	770	12	CDOM, Chl.a, Pigment, Nutrients	0*	10	15*	20	40*	60*	80	100*	300*	500*	600*	700*	
28	630	12	Chl.a, Pigment, Nutrients	0	20	40	60	80	100							
32	626	11	Chl.a, Pigment, Nutrients	0	20	40	60	80	100							

* CDOM sampling depth.

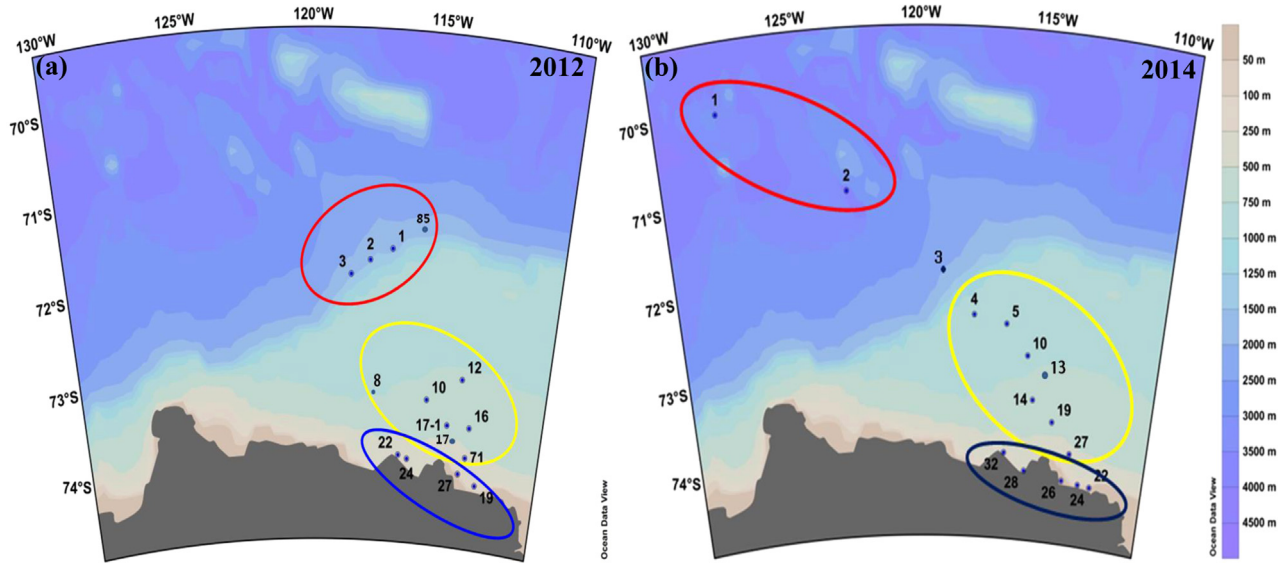

Fig. 1. Locations of the stations during austral summer in 2012 (a) and 2014 (b) cruise. Sea ice zone, Amundsen Sea Polynya, and ice shelf stations were indicated by red circles, yellow circles, and blue circles, respectively. (For interpretation of the references to color in this figure legend, the reader is referred to the web version of this article).

(w/w). The contribution of the three marker pigments to Chl-a was determined using the approach described by Everitt et al. (1990).

$$\text{diatoms Chl a} = 0.9[\text{fuco} - 0.05\ (\text{hex} - \text{fuco})] \quad (1)$$

$$\textit{Phaeocystis spp.}\ \text{Chl a} = 1.25\ (\text{hex} - \text{fuco}) \quad (2)$$

$$\text{cryptophytes Chl a} = 0.7\ (\text{allo}) \quad (3)$$

The coefficient 0.05 was included in the diatoms algorithm to correct for the fact that *Phaeocystis* spp. also contained some fuco (Tyler, 1975).

2.4. CDOM analysis

Seawater samples (250 mL) were taken using a CTD rosette sampler equipped with Niskin bottles. Immediately seawater samples were filtered through pre-cleaned 0.2 μm membrane filters for measurements of CDOM absorption and stored in glass bottles. The glass bottles are autoclaved in 400 °C. All samples were stored frozen in darkness for later analysis. CDOM absorbance was measured on a Cary-100 UV–vis spectrophotometer using a 10 cm quartz cuvette and Milli-Q water as a reference. Spectra were measured from 200 to 800 nm every 0.5 nm in triplicate and then averaged. The optical density acquired from the instrument was converted to the CDOM absorption coefficient ($a_{CDOM}(\lambda)$) using the following equation.

$$a(\lambda) = 2.303 \times \frac{A(\lambda)}{l}$$

$$a(\lambda) = a(\lambda_0)\exp[-S(\lambda-\lambda_0)]$$

$a(\lambda)$: absorption coefficient (m^{-1}), $a(\lambda_0)$: absorption coefficient at reference wavelength (m^{-1}), $A(\lambda)$: optical density at a given wavelength λ, 2.303: conversion factor from $\log_{10}$ to log units, l: length of optical path (m), S: slope coefficient (μm^{-1})

The CDOM absorption spectrum typically declines exponentially with wavelength when measured from 300 to 500 nm and, hence, can be modeled as an exponential function of wavelength (Bricaud et al., 1981). The modeled exponential S value of this spectrum offers an indication of CDOM quality because it varies depending on its source, age, and extent of degradation (Carder et al., 1989). The shape of the absorption spectra between 300 nm and 500 nm was characterized by determining the exponential S value according to the approach by Stedmon et al. (2011). We reported the average values of CDOM and S values for SIZ, ASP and IS. And, the CDOM and S values for upper and lower water column ranged from euphotic depth were also compared for regional differences. The euphotic depth was defined as the depth at 1% penetration of surface photosynthetically active radiation (PAR).

2.5. Nutrients

Seawater sampling for nutrients was carried out at 15 stations throughout the Amundsen Sea in 2014 (ANA04B) using a CTD rosette sampler holding 24–10 L Niskin bottles (Ocean Test Equipment Inc., FL, USA). Nutrients samples were collected from the Niskin rosette into 50 mL conical tubes and immediately stored in a refrigerator at 2 °C prior to chemical analyzes. Inorganic macronutrient [$NO_3(=NO_2+NO_3)$, PO_4, SiO_2 and NH_4] concentrations were determined onboard ship using an Auto-Analyzer system (QuAAtro, Seal Analytical) according to the Joint Global Ocean Flux Study (JGOFS) protocols described by Gordon et al. (1993).

2.6. Nutrient disappearances

We used nutrient concentrations at the 500 m depth, as a proxy for the pre-bloom concentrations within the upper 100 m. The disappearance of nutrients at each sampling depth was calculated as the difference between the observed concentration and the concentration of 500 m depth value. These differences were used to estimate the disappearances (Δ) of NO_3 (ΔNO_3), PO_4 (ΔPO_4), and SiO_2 (ΔSiO_2) within the upper 100 m of the water column.

2.7. Statistical analyzes

Statistical analyzes were performed with IBM SPSS 21.0 (Statistical program for Science). Differences in response between two categories were assessed with a two sample t-test, using a p-Value of 0.05 or 0.01 to determine statistical significance. Differences of three parameters were assessed with analyzes of variance (ANOVA). Correlation analyzes were used to examine the relationship between variables using SPSS.

3. Results

3.1. ANA02C cruise (2012)

3.1.1. Chlorophyll a

In ANA02C cruise (2012), concentrations of Chl-a ranged from 0.04 to 4.34 μg L^{-1} and the average of Chl-a concentrations in the upper 100 m of the water column was 1.56 ± 1.04 μg L^{-1} [mean ± standard deviation (SD)] (Table 2). The highest Chl-a concentration (4.34 μg L^{-1}) was found at the ASP and the lowest Chl-a concentration was found at SIZ in a relatively high sea ice coverage site (Fig. 2a). The average concentrations Chl-a at the surface in the ASP (2.31 ± 1.01 μg L^{-1}) was relatively higher than in the SIZ (1.10 ± 0.61 μg L^{-1}) and IS (0.67 ± 0.15 μg L^{-1}). The Chl-a concentrations were significantly different ($F=18.92$, $v=2$, $p<0.01$) among the SIZ, ASP, and IS. In addition, statistical differences were observed in the ASP-SIZ and SIZ-IS (post-hoc, $p<0.001$). Maximum Chl-a concentration was observed near the surface layer at most of the stations.

3.1.2. Taxonomy and composition of phytoplankton

(1) *Phytoplankton taxa*
The accessory pigments detected by HPLC analysis of seawater samples collected during austral summer in ANA02C were Chl-b, Chl-c_2, Chl-c_3, hex-fuco, fuco, allo, perid, viola, zea, lut, but-fuco, DD and DT. Based on the marker pigments, the major phytoplankton groups were prymnesiophytes and diatoms and the minor groups were cryptophytes, chlorophytes, dinophytes, chrysophytes and cyanophytes (Smith et al., 2010). At all stations, fuco and hex-fuco were present revealing the presence of diatoms and prymnesiophytes in ANA02C. Among the prymnesiophyte, *P. antarctica* was confirmed as major phytoplankton by microscopic observation (Yang et al., 2013) and the biomarker was hex-fuco (Buma et al., 1991). Allo was used as marker for cryptophytes, which were present at low salinity stations in ANA02C.

(2) *The hex-fuco: Chl-a and fuco: Chl-a ratios*
The hex-fuco:Chl-a ratios ranged from detection limit to 0.72 and the highest average of ratio observed in the ASP

Table 2
Chlorophyll a concentrations during austral summer in the Amundsen Sea in both 2012 and 2014.

	2012			2014		
Chl a (μg/L)[a] (± SD)	**1.56** (± 1.04)			**2.40** (± 2.42)		
Range	0.04–4.34			0.10–12.64		
Region	SIZ	ASP	IS	SIZ	ASP	IS
Chl a(μg/L)[b] (± SD)	**1.10** (± 0.61)	**2.31** (± 1.01)	**0.67** (± 0.15)	**0.17** (± 0.04)	**3.92** (± 3.14)	**2.21** (± 0.37)

[a] average value integrated from the surface to 100 m.
[b] average of the surface value.

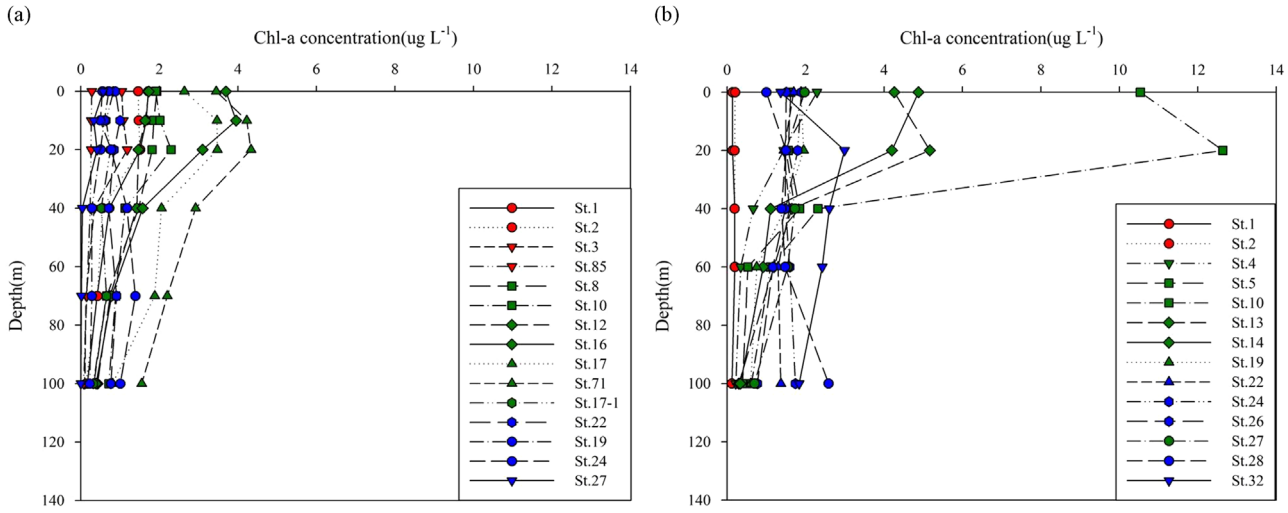

Fig. 2. Vertical patterns in chlorophyll a concentrations (μg L^{-1}) from the surface to 100m depth at all stations during austral summer in both 2012 (a) and 2014 (b). Sea ice zone, Amundsen Sea Polynya, and ice shelf stations were indicated by red color, green color, and blue color, respectively. (For interpretation of the references to color in this figure legend, the reader is referred to the web version of this article).

Table 3
The average hex-fcuo:chl-a and fuco:chl-a ratios integrated from the surface to 100 m in the SIZ, ASP and IS in both 2012 and 2014.

	SIZ		ASP		IS	
	2012	2014	2012	2014	2012	2014
Hex-fuco: Chl-a*(w/w) (± SD)	**0.36** (± 0.16)	**0.18** (± 0.09)	**0.47** (± 0.11)	**0.29** (± 0.10)	**0.28** (± 0.10)	**0.20** (± 0.04)
Fuco: Chl-a*(w/w) (± SD)	**0.25** (± 0.12)	**0.24** (± 0.15)	**0.10** (± 0.03)	**0.14** (± 0.09)	**0.11** (± 0.05)	**0.09** (± 0.01)
Hex-fuco/ Fuco*	**1.4**	**0.75**	**4.7**	**2**	**2.5**	**2.2**

* The average values of multiple stations for each SIZ, ASP and IS.

(0.47 ± 0.11), which was higher than in the SIZ (0.36 ± 0.16) and IS (0.28 ± 0.11) (Table 3). The hex-fuco:Chl-a ratios were significantly different ($F=11.106$, $v=2$, $p<0.01$) among three regions. And, significant differences were found at the ASP-SIZ (post-hoc, $p<0.05$) and the SIZ-IS (post-hoc, $p<0.01$). The fuco:Chl-a ratios from the surface to 100 m ranged from 0 to 0.49. The average ratio in the SIZ (0.25 ± 0.12) was higher than in the ASP (0.10 ± 0.03) and IS (0.11 ± 0.05) (Table 3). The fuco: Chl-a ratios were significantly different ($F=24.291$, $v=2$, $p<0.01$) among the SIZ, ASP and IS. Furthermore, significant differences were found at the ASP-SIZ (post-hoc, $p<0.01$) and the SIZ-IS (post-hoc, $p<0.01$). Compared to two major pigments, the hex-fuco/fuco ratios ranged from 1.4 to 4.7, suggesting that hex-fuco was the dominant pigment than fuco during study period of 2012.

(3) *Compositions of major phytoplankton group*

The largest phytoplankton bloom was dominated by *P. antarctica*, which was located in the ASP (90%) and IS (80%). However, in the SIZ, *P. antarctica* comprised 62% of phytoplankton composition, which was relatively lower than the ASP and IS (Fig. 3a). Proportion of diatoms accounted for 36% of the average phytoplankton composition in the SIZ. In the ASP and IS, diatoms accounted for 28% and 23% of the phytoplankton group. The cryptophytes was found near the surface, which was a very small bloom in our study (less than 1%).

3.2. ANA04B cruise (2014)

3.2.1. Chlorophyll a

In ANA04B cruise, Chl-a concentration in the upper 100 m of the water column ranged from 0.10 to 12.64 μg L^{-1} and the average of Chl-a was 2.40 ± 2.42 μg L^{-1} (Table 2). The highest Chl-a concentration was found at the ASP and the lowest Chl-a concentration was found at SIZ (Fig. 2b). The average concentration of Chl-a at the surface in the ASP (3.92 ± 3.14 μg L^{-1}) was relatively higher than in the SIZ (0.17 ± 0.04 μg L^{-1}) and IS (2.21 ± 0.37 μg L^{-1}). Concentrations of Chl-a were significantly different ($F=7.44$, $v=2$, $p<0.01$) among the SIZ, ASP and IS. Especially, concentrations of Chl-a were statistically different between the ASP and SIZ (post-hoc, $p<0.001$). Like in ANA02C cruise, maximum Chl-a concentration was observed near the surface layer, the 20–40 m depth at most of the stations.

3.2.2. Taxonomy and composition of phytoplankton

(1) *Phytoplankton taxa*

The accessory pigments also detected by HPLC analysis of seawater samples collected during austral summer in ANA04B were Chl-b, Chl-c_2, Chl-c_3, hex-fuco, fuco, allo, perid, viola, zea, lut, but-fuco, DD and DT. Based on the marker pigments, the major phytoplankton groups were prymnesiophytes and diatoms and the minor groups were cryptophytes, chlorophytes, dinophytes, chrysophytes and cyanophytes. At all stations, fuco and hex-fuco were present revealing the presence of diatoms and prymnesiophytes in ANA04B. Among the prymnesiophyte, *P. antarctica* was confirmed as major phytoplankton by microscopic observation (Yang et al., 2013) and the biomarker was hex-fuco (Buma et al., 1991). Allo was used as marker for cryptophytes, which were present at low salinity stations in ANA04B.

(2) *The fuco: Chl-a and hex-fuco: Chl-a ratios*

The hex-fuco:Chl-a ratios ranged from below detection limit to 0.47 and the average ratio in the ASP (0.29 ± 0.10) was higher than in the SIZ and IS (0.18 ± 0.09 and 0.20 ± 0.04) (Table 3). And, the hex-fuco:Chl-a ratios were significantly different ($F=11.949$, $v=2$, $p<0.01$) among three regions. The fuco:Chl-a ratios from the surface to 100 m depth ranged from 0.04 to 1.22 (Table 3). The average ratio of fuco : Chl-a in the SIZ (0.24 ± 0.15) was higher than in the ASP and IS (0.14 ± 0.09

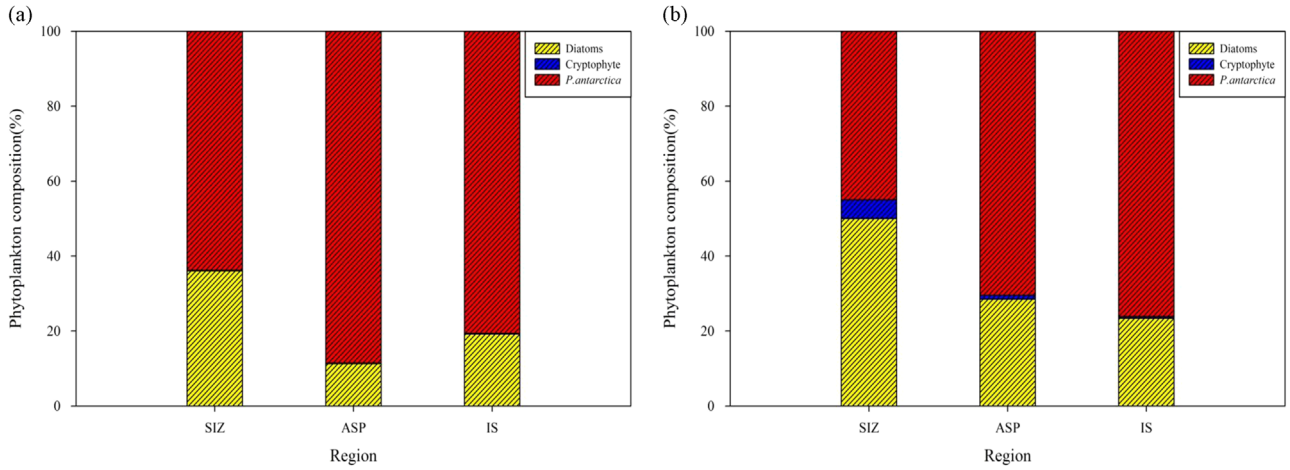

Fig. 3. The average phytoplankton major groups composition at different region (multiple stations with each zone) during austral summer in both 2012 (a) and 2014 (b). Diatoms, *P. antarctica* and cryptophytes indicated by red bar, yellow bar, and blue bar. (For interpretation of the references to color in this figure legend, the reader is referred to the web version of this article)

and 0.09 ± 0.01). The fuco:Chl-a ratios were significantly different ($F=4.267$, $v=2$, $p<0.05$) among the SIZ, ASP and IS. Significant differences were found in the SIZ-IS (post-hoc, $p<0.01$) and ASP-IS (post-hoc, $p<0.05$). Generally fuco:Chl-a ratio in the SIZ was higher than hex-fuco:Chl-a ratio, but they were not significantly different ($t=0.859$, $v=32$, $p>0.05$). Hex-fuco/fuco ratios ranged from 0.75 to 2.2. The high ratio of hex-fuco/fuco (>2) implies that hex-fuco was dominant pigment in the ASP and IS.

(3) *Compositions of major phytoplankton group*

The largest phytoplankton bloom was dominated by *P. antarctica* and was located in the ASP (70%) and IS (76%) (Fig. 3b). Diatoms were always observed in association with *P. antarctica* in our study area, but at low densities, except in the SIZ. Diatoms accounted for 50% of the average phytoplankton composition in the SIZ, which was relatively higher than that of the ASP (28%) and IS (23%). Cryptophytes was a very small bloom in the Amundsen Sea, accounted for 5% of the average phytoplankton composition in the SIZ and less than 1% in the ASP and IS.

3.2.3. Nutrients

(1) *Distribution of Nutrients*

Nutrient concentrations were obtained for six sampling depths from the surface to 100 m in January, 2014 and vertical profiles of each nutrient are shown in Fig. 4. The NO_3 concentration in the Amundsen Sea ranged from 3.47–31.25 μM from the surface to 100m depth and peaked in deep water (60 to 100 m) at all stations (Fig. 4a). The NO_3 concentrations at the surface were lower in the ASP compared to SIZ and IS, and vertical distribution showed large variation (8.96–31.25 μM). The PO_4 concentration ranged from 0.57–2.17 μM in the water column (Fig. 4b). The PO_4 concentrations at the surface were the lowest in the ASP (0.58–1.45 μM), and vertical distribution showed large variation (0.58–2.11 μM). Most of the NO_3 and PO_4 concentrations gradually increased with depth and the vertical patterns were very similar each other. We found that the concentration of NO_3 in the water column was well correlated with that of PO_4 in the Amundsen Sea ($r^2=0.94$, $p<0.05$). The NO_3 and PO_4 concentrations were significantly different ($F=6.75$ and 6.41, $v=2$, $p<0.01$) among the SIZ, ASP and IS, especially the SIZ-ASP and the SIZ-IS (post-hoc, $p<0.01$).

The SiO_2 was homogeneously distributed from the surface to 100 m at all station, except station 4 and 5. The range of SiO_2 was 56.10–89.60 μM (Fig. 4c) and high SiO_2 concentrations (>75.00 μM) were observed in most of the ASP and IS. NH_4 concentrations were very low (<1.6 μM) throughout the water column (Fig. 4d) and no distinct spatial pattern was observed in the water column. The range of NH_4 was 0.0–1.6 μM and peak from 40 to 100 m at all stations. Especially, rapid increase of NH_4 concentration was observed between 20 and 80 m depth of station 32.

(2) *N:P drawdown ratio*

The disappearance of nutrients at each sampling depth was calculated as the difference between the observed concentration and the concentration at 500 m depth value (Table 4). Assuming a pre-bloom NO_3 concentration as 35.30 μM, the highest average ΔNO_3 was 14.49 μM (± 8.3 μM) in the ASP, where dominated by *P. antarctica* (Table 4). The average disappearance of NO_3 concentrations in ASP was approximately 50% of pre-bloom concentrations. The average of ΔNO_3 in the ASP was statistically higher ($t=4.851$, $v=58$, $p<0.01$) than in the SIZ (5.56 ± 0.78 μM), where dominated by diatoms. Assuming the pre-bloom concentration of PO_4 was 2.48 μM in the upper 100 m, the highest average ΔPO_4 was 0.89 ± 0.62 μM in the ASP, where dominated by *P. antarctica* and was statistically higher ($t=4.089$, $v=51$, $p<0.01$) than SIZ, where diatoms were dominant. The highest disappearance of NO_3 and PO_4 were found in the ASP, where dominated by *P. antarctica* and were significantly different ($F=7.23$ and 7.11, $v=2$, $p<0.01$) among the SIZ, ASP and IS. When pre-bloom concentration of SiO_2 is assumed as 94.5 μM, the ΔSiO_2 in the SIZ was 26.61 ± 5.39 μM, which is much higher than in the ASP and IS. This suggested that higher proportion of diatoms in the composition of phytoplankton community, which has a high requirement of SiO_2 in the SIZ, compared to the ASP and IS.

The average ΔNO_3:ΔPO_4 ratio within the euphotic layer (Table 4) was 16:1 in the ASP and IS, where dominated by *P. antarctica*. This ratio was similar to the Redfield ratio of 16:1, but lower than ΔNO_3:ΔPO_4 ratio of *P. antarctica* (19:1) in the Southern Ocean reported by Arrigo et al. (2000). However, in the SIZ dominated by diatoms, the ΔNO_3:ΔPO_4 ratio was 15:1, which is higher than the 10:1 ratio reported by Arrigo et al. (2000) from Ross sea when diatom was dominant. This seems to be the result of the mixed population of phytoplankton in 2014. Although *P. antarctica* was predominant, representing over 70% of the phytoplankton community on average, diatoms always composed ~20% of phytoplankton assemblages in our study area of the Amundsen Sea.

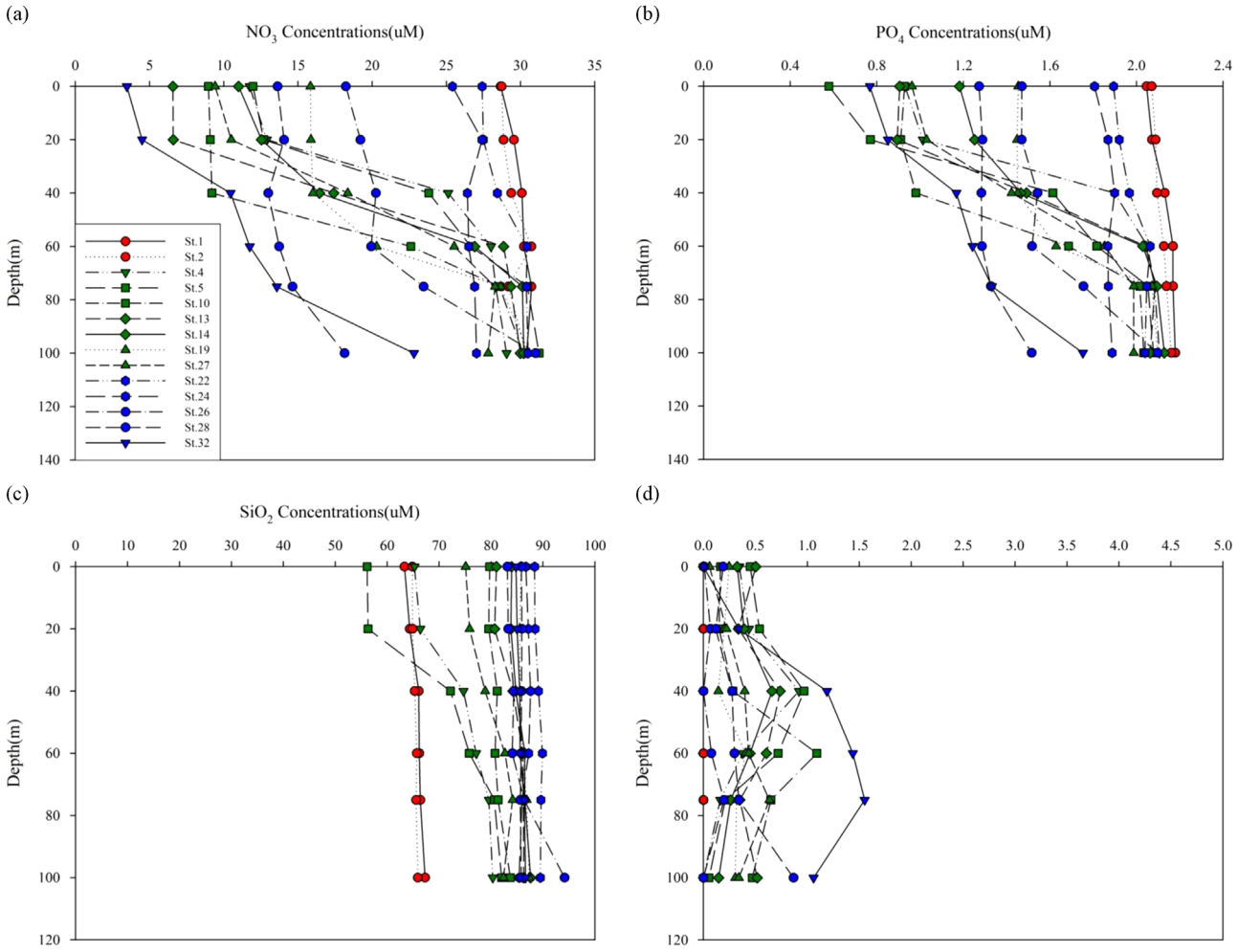

Fig. 4. The vertical profiles of nutrients concentrations (μM) during austral summer in the Amundsen Sea in 2014. sea ice zone stations were indicated by red color, Amundsen Sea Polynya and ice shelf stations were indicated by green and blue color (a:NO_3, b:PO_4, c:SiO_2, d:NH_4). (For interpretation of the references to color in this figure legend, the reader is referred to the web version of this article).

Table 4
The mean of disappearance each nutrients from 6 sampling depth and the average of disappearance N:P ratios integrated from the surface to 100 m in the Amundsen Sea in 2014 (multiple stations with each zone).

	Disappearance of nutrients (Mean ± SD μM)								
	SIZ			ASP			IS		
	ΔNO_3	ΔPO_4	ΔSiO_2	ΔNO_3	ΔPO_4	ΔSiO_2	ΔNO_3	ΔPO_4	ΔSiO_2
0	**6.61** (±0.04)	**0.42** (±0.02)	**31.27** (±1.66)	**24.51** (±0.91)	**1.49** (±0.27)	**19.21** (±8.85)	**17.67** (±9.66)	**1.04** (±0.45)	**8.73** (±1.97)
20	**6.10** (±0.49)	**0.40** (±0.01)	**29.51** (±0.74)	**23.84** (±3.01)	**1.43** (±0.23)	**19.06** (±9.15)	**16.76** (±8.70)	**1.00** (±0.44)	**8.53** (±1.98)
40	**5.57** (±0.51)	**0.37** (±0.01)	**26.08** (±4.75)	**17.24** (±5.30)	**1.01** (±0.27)	**14.28** (±5.21)	**15.58** (±7.94)	**0.91** (±0.36)	**8.01** (±1.88)
60	**4.82** (±0.36)	**0.33** (±0.03)	**24.63** (±6.82)	**9.75** (±3.06)	**0.61** (±0.17)	**12.36** (±3.06)	**14.83** (±8.02)	**0.88** (±0.33)	**7.98** (±2.19)
75	**5.35** (±0.82)	**0.33** (±0.02)	**24.14** (±7.62)	**6.19** (±0.88)	**0.42** (±0.04)	**10.89** (±3.05)	**13.50** (±7.44)	**0.81** (±0.32)	**7.71** (±1.61)
100	**4.91** (±0.02)	**0.31** (±0.01)	**24.00** (±6.78)	**5.43** (±1.12)	**0.41** (±0.05)	**10.25** (±2.87)	**9.40** (±3.21)	**0.62** (±0.23)	**6.79** (±2.50)
Range	**4.57–17.25**	**0.30–1.43**	**27.22–31.17**	**4.05–28.72**	**0.35–1.90**	**6.89–38.35**	**4.30–31.82**	**0.38–1.71**	**3.34–11.35**
Mean	**5.56** (±0.78)	**0.36** (±0.04)	**26.61** (±5.39)	**14.49** (±8.3)	**0.89** (±0.62)	**14.34** (±7.49)	**14.62** (±7.91)	**0.88** (±0.36)	**8.19** (±1.96)

*integrated from the surface to euphotic layer.

3.2.4. CDOM

(1) *Distribution of CDOM*

The a_{355} values in our study ranged from 0.07 to 0.98 m^{-1} with the highest values recorded in the euphotic layer of the ASP (Fig. 5a). The vertical distribution of a_{355} values showed large variation in the ASP than that of the SIZ and IS (Fig. 5b). At depths deeper than the ED, a_{355} values generally remained below 0.4 m^{-1}. The average value of a_{355} in the euphotic layer (0.26 ± 0.09 m^{-1}) was higher than that of below the ED (0.18 ± 0.02 m^{-1}), which was significantly different ($t=3.11$, $\nu=63$, $p<0.05$).

In the euphotic layer, the average values of a_{355} were 0.51 m^{-1} in the ASP, 0.10 m^{-1} for SIZ and 0.16 m^{-1} for IS (Table 5). And, the a_{355} values were significantly different ($F=16.67$, $\nu=2$, $p<0.01$) among the three regions. Especially, significant

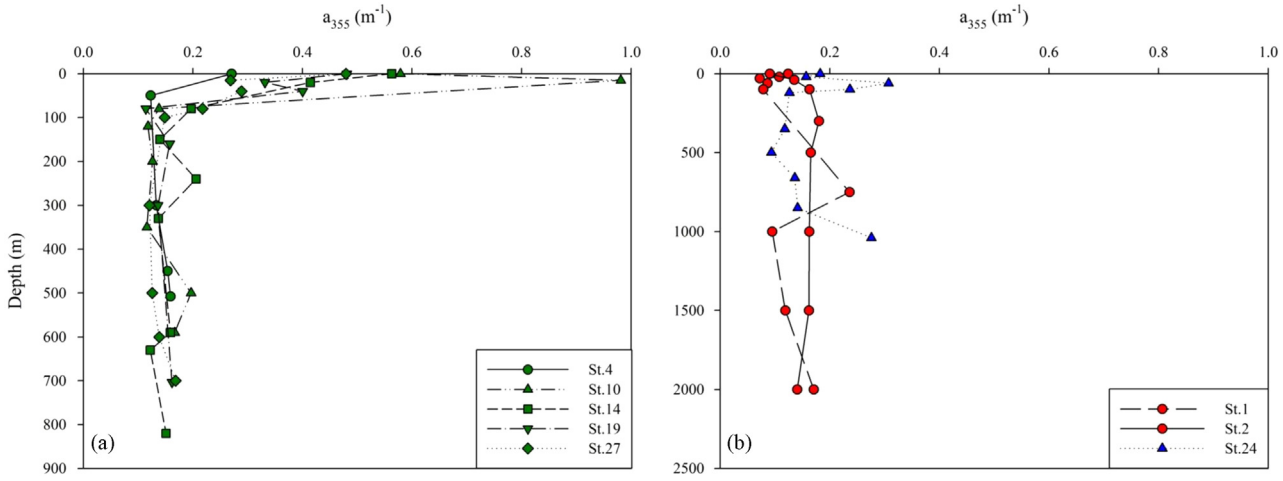

Fig. 5. Vertical patterns in a_{355} (m^{-1}) in the Amundsen Sea Polynya (a), and in the sea ice zone and ice shelf (b) during austral summer in 2014.

Table 5
The average a_{355} (m^{-1}) and $S_{300-500}$ (μm^{-1}) values integrated from the surface to the euphotic layer and below the euphotic depth in the Amundsen Sea in 2014.

		SIZ*	ASP*	IS*	Mean
a_{355}(m^{-1}) (±SD)	Euphotic layer	**0.10** (±0.02)	**0.51** (±0.19)	**0.16** (±0.01)	**0.26** (±0.09)
	Below Euphotic layer	**0.14** (±0.04)	**0.24** (±0.07)	**0.17** (±0.08)	**0.18** (±0.02)
$S_{300-500}$(μm^{-1}) (±SD)	Euphotic layer	**13** (±2)	**14** (±4)	**19** (±10)	**15** (±4)
	Below Euphotic layer	**10** (±3)	**15** (±3)	**11** (±1)	**11** (±1)

* The average values of multiple stations for each SIZ, ASP and IS.

differences of the a_{355} values were found in the ASP-SIZ (post-hoc, $p<0.01$) and SIZ-IS (post-hoc, $p<0.05$). Below the ED, the average values of the a_{355} were 0.24 m^{-1} in the ASP, 0.14 m^{-1} for the SIZ and 0.17 m^{-1} for IS (Table 5) and the average value of a_{355} in the ASP was higher than other regions. Unlike the euphotic layer, however, the a_{355} values were not significantly different among the SIZ, ASP and IS ($F=1.05$, $v=2$, $p>0.05$). The a_{355} values slightly increased from the euphotic layer to below the ED in the SIZ and IS, but the a_{355} values in the ASP decreased (Table 5). The a_{355} values between the euphotic layer and below the ED were significantly different in the SIZ ($t=2.335$, $v=13$, $p<0.05$) and ASP ($t=6.49$, $v=34$, $p<0.01$), but there were not significantly different in the IS ($t=0.163$, $v=8$, $p>0.05$).

(2) *Relationship between CDOM and various factors*

The relationship between Chl-a and a_{355} values has been used in our study to determine the link between increased Chl-a concentrations and the production of CDOM. A positive linear relationship was observed between average a_{355} values and Chl-a in the Amundsen Sea during austral summer. Thus, high a_{355} values were well correlated with high Chl-a concentrations ($r^2=0.70$, $n=30$, $p<0.05$) (Fig. 6a). In contrast, no significant relationship was observed between salinity and average a_{355} values ($r^2=-0.01$, $n=67$, $p>0.05$) (Fig. 6b). In order to find the main source of CDOM production by among different taxa of phytoplankton, regression analyzes between a_{355} and marker pigments of (hex-fuco) major phytoplankton was performed. Significant linear correlations were found between a_{355} and pigment concentration for fuco ($r^2=0.31$, $n=30$, $p<0.05$) (Fig. 7a) and hex-fuco ($r^2=0.78$, $n=30$, $p<0.05$) (Fig. 7b), but the stronger correlation with hex-fuco, indicates that *P. antarctica* was more important to CDOM production than diatoms in our study area.

3.2.5. S value

Spectral slopes ($S_{300-500}$) in our study varied from 6 to 28 μm^{-1}. The average values of $S_{300-500}$ in the euphotic layer and below the ED were 15 μm^{-1} (±4 μm^{-1}) and 11 μm^{-1} (±1 μm^{-1}), respectively (Table 5). However, the $S_{300-500}$ values were not significantly different between euphotic layer and below the ED ($t=0.397$, $v=63$, $p>0.05$).

In the euphotic layer, the $S_{300-500}$ values 19 μm^{-1} (±10 μm^{-1}) in IS, 14 μm^{-1} (±4 μm^{-1}) for the ASP and 13 μm^{-1} (±2 μm^{-1}) for the SIZ. The average value of $S_{300-500}$ in IS was higher than other regions, but they were not statistically different ($F=0.84$, $v=2$, $p>0.05$) (Table 5). Below the ED, the average values of $S_{300-500}$ were 15 μm^{-1} (±3 μm^{-1}) in the ASP, 10 μm^{-1} (±3 μm^{-1}) for SIZ and 11 μm^{-1} (±1 μm^{-1}) for IS (Table 5). However, the $S_{300-500}$ values were not significantly different ($F=2.33$, $v=2$, $p>0.05$) among the SIZ, ASP and IS.

4. Discussion

4.1. Chlorophyll a

In our study, the highest Chl-a concentration was observed at the ASP in both February 2012 and January 2014. The average concentration of Chl-a in the ASP was approximately two or three (February 2012) and two of twenty (January 2014) times higher than in the SIZ and IS (Table 2). In addition, the highest Chl-a concentration in the water column (Fig. 2) were all located in the moderately fresh Antarctic surface water (AASW) layer in the central ASP, where sea ice melt signature were found enhancing stratification (mixed layer depth <30 m) and increasing light availability. Shallow mixed layer depth is related to sea ice melt, which freshen the surface, including shallow stratification that subsequently warms by increased insolation (Yager et al., 2012). In our study, positive relationship between phytoplankton biomass and enhanced stratification was observed, suggesting an important role for light availability in phytoplankton bloom formation. Thus, the phytoplankton biomass is influenced by solar radiation after sea ice melting. The average concentration of Chl-a in the ASP was similar with the previously reported by Alderkamp et al. (2012) (4.33 $\mu g L^{-1}$) and Lee et al. (2012) (3.95 $\mu g L^{-1}$), which was substantially more productive than in the SIZ and IS in the Amundsen Sea.

Arrigo and van Dijken (2003) reported that Chl-a concentrations in the Amundsen Sea increase in response to increasing solar

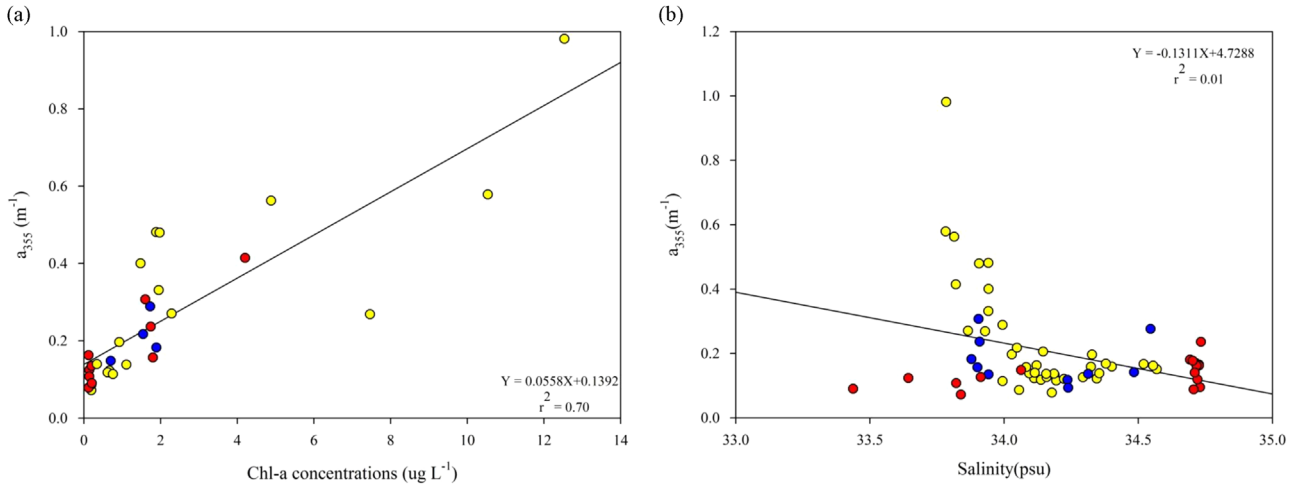

Fig. 6. The scatter plot of chlorophyll a concentration (μg L^{-1}) (a) and salinity (psu) (b) with a_{355} (m^{-1}) during austral summer in the Amundsen Sea. Sea ice zone, Amundsen Sea Polynya and ice shelf stations were indicated by red circle, yellow circle, and blue circle respectively. (For interpretation of the references to color in this figure legend, the reader is referred to the web version of this article).

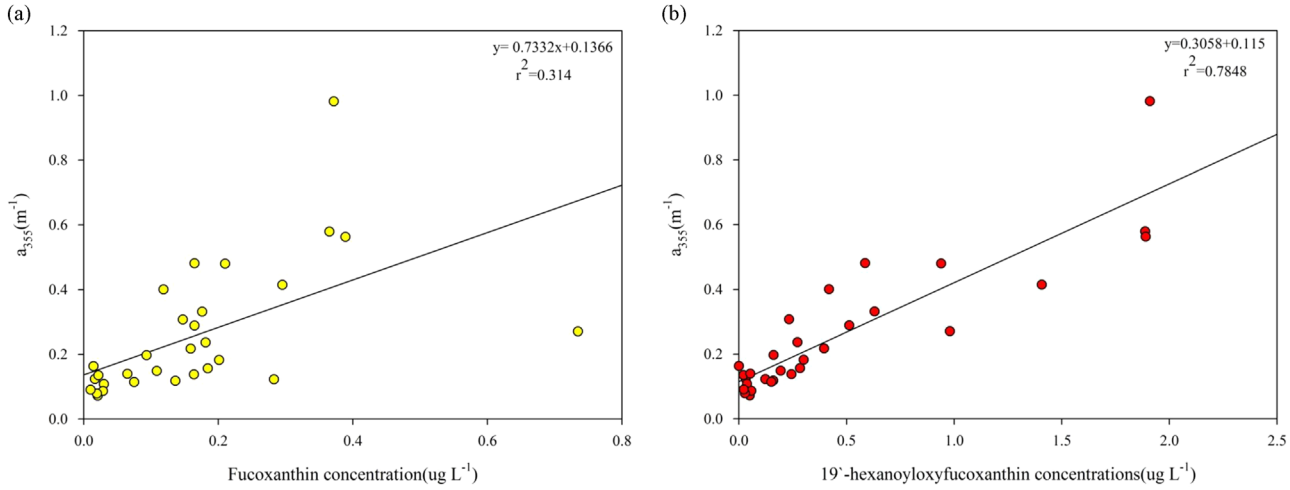

Fig. 7. The scatter plot of fucxanthin concentration (μg L^{-1}) versus a_{355} (m^{-1}) (a) and 19′-hexanoyloxyfucoxanthin (μg L^{-1}) versus a_{355} (m^{-1}) (b) during austral summer (2014) in the Amundsen Sea.

radiation in October, peak during austral summer in January, begin to decrease in February, and reach post-bloom by March. Also, Arrigo and van Dijken (2003) and Lee et al. (2012) reported three-fold decreases in *in situ* primary productivity from the early bloom period in January to the termination period. Hahm et al. (2014) reported a strong temporal variation of mean net community production (NCP) in the Amundsen Sea during January, 2011 and February, 2012. The author explained that the mean net community production (NCP) in February 2012 was 19% of the NCP from January 2011. Sampling period of our two cruise coincide with declining bloom period (first, February 2012) and peak bloom period (second, January 2014), respectively. Our result in February 2012 showed that the average concentration of Chl-a was about 65% of in January 2014. The average of Chl-a in the ASP was approximately 58% of the Chl-a at the ASP in January 2014. In addition, peak bloom conditions in January 2014 showed very high concentration of Chl-a up to 12.64 μg L^{-1} at the center of the ASP and Chl-a distribution showed large variation (0.10–12.64 μg L^{-1}). However, in February 2012, the range of Chl-a was moderate and the variation (0.04–4.34 μg L^{-1}) was smaller than in January 2014. Moreover, Chl-a concentrations from surface to 100m depth were significantly different ($t=2.508$, $v=180$, $p<0.05$) between February 2012 and January 2014.

4.2. Taxonomy and composition of phytoplankton

The phytoplankton groups detected in the Amundsen Sea was quite diverse: two major groups for prymensiophytes, diatoms minor groups of cryptophytes, dinophytes, chrysophytes, chlorophytes and cyanophytes. During two cruise, *P. antarctica* showed the widest distribution and highest biomass of Chl-a, which extended from the ASP to IS in February 2012 and January 2014. In February 2012, the hex-fuco:Chl-a ratio in the upper 100 m of the water column was higher than the fuco:Chl-a ratio (Table 3). According to hex-fuco/fuco ratios in January 2014 and February 2012, predominance (> 1.5) of *P. antarctica* was dominant at all study areas, except the SIZ in January 2014. However, the maximum relative ratio of Hex-fuco in ASP was increased from 2.0 at early summer (peak bloom season) in January 2014 to 4.7 at late summer (declining bloom season) in February 2012.

In contrast *P. antarctica* was dominant phytoplankton taxa at the ASP and IS, relative proportion of *P. antarctica* and diatoms was comparable at the SIZ in both February 2012 and January 2014. In the SIZ, diatoms and *P. antarctica* were approximately equally abundant, composing 40%:60% (February 2012) and 51%:45% (January 2014) of the phytoplankton biomass. The hex-fuco/fuco ratios were 1.4 (February) and 0.75 (January), which is showing

that the dominant phytoplankton group changed from diatoms in January to *P. antarctica* in February. Although *P. antarctica* biomass was dominant at the most of stations in our study area, diatoms was dominated at the fringe in January 2014 (marginal ice zone), where located in the boundary at the ASP. In general, diatoms are known to be dominant at the retreat ice edge of marginal ice zone.

Buma et al. (1992) reported high allo concentrations in the Bellingshausen Sea and explained that cryptophytes could dominate the phytoplankton biomass near the retreating sea ice. Our result showed also a moderate abundance of cryptophytes, which are known to favor low saline water. Cryptophytes was observed only in the offshore region in January 2014 (Fig. 3b), which indicated the presence of sea ice melt water and lower salinity in this region.

4.3. Nutrients and the N:P drawdown ratio

In the ocean, nutrients provide compounds necessary for phytoplankton blooms, and in combination with light, nutrients have been shown to limit phytoplankton growth. The inferred removal of nutrients was integrated from the surface to 100 m. In general, high phytoplankton biomass was associated with high ΔNO_3 and ΔPO_4. Disappearance of NO_3 and PO_4 was highest in the ASP and IS, which were dominated by *P. antarctica*. Disappearance of NO_3 and PO_4 was relatively low in the SIZ, where dominated by diatoms. These results are well correlated with the phytoplankton assemblages in each region. Unlike ΔNO_3 and ΔPO_4, ΔSiO_2 was highest in the SIZ and the outer shelf region and was very low at the ASP and IS in austral summer. Priddle et al. (1998) reported that the average annual changes in the concentrations of SiO_2, PO_4, and NO_3 were 10–20 μM, 0.5–0.75 μM, and 5–10 μM, respectively, in the Southern Ocean. Our nutrient removal values of SiO_2 and PO_4 (SiO_2 : 8.19–26.61 μM, PO_4 : 0.36–0.89 μM) were similar to the previous data, but ΔNO_3 were relatively higher (NO_3: 5.56–14.62 μM) in the ASP and IS than in other regions of the Southern Ocean.

Weber and Deutsch (2010) reported that large scale variability in nutrient uptake ratios stem primarily from the relative abundance of species with distinct requirements. Species driven deviation from the Redfield ratio (16:1 for N:P) has been reported in the Southern Ocean: in the coastal waters of the Ross Sea the local balance of low disappearance N:P due to diatoms and high disappearance N:P due to *P. antarctica* was found to maintain an N:P export ratio 16:1 on relatively small scales. Arrigo et al. (2000) suggested that the N:P disappearance ratios for waters by *P. antarctica* was 19.0 ± 0.89, which was higher than that of diatoms-dominated waters (9.52 ± 0.81). The variance of the N:P ratio is governed by regional differences in the species composition of the phytoplankton community (Weber and Deutsch, 2010). The N:P drawdown ratio was higher in *P. antarctica*-dominated waters (16:1) than in diatoms-dominated waters (15:1). Our results from mixed populations of *P. antarctica* and diatoms revealed averaged N:P drawdown ratios integrated from the surface to 100m of 15:1 (SIZ) and 16:1 (ASP and IS) (Table 4). The reason for this result may be relatively higher composition of diatoms in our study area (23–28%) compared to the Ross Sea (less than 5%). Also, the N:P drawdown ratio was higher in *P. antarctica*-dominated waters than in diatoms-dominated waters, indicating that *P. antarctica* may have a higher uptake and biological requirement for N than diatoms (Arrigo et al., 2000).

4.4. CDOM

We reported the high CDOM values (a_{355}) in the ASP during summer expedition of ANA04B (January 2014) (Table 5) which was significantly higher than in the SIZ. The average values of a_{355} were significantly different ($t=3.11$, $\nu=63$, $p<0.05$) between the euphotic layer and below the ED among the SIZ, ASP and IS. The average of CDOM value in the ASP is equivalent 1.2 m^{-1} at 300 nm and 1.07 m^{-1} at 325 nm, which is exceptionally higher than 0.39 m^{-1} any other regions of the Antarctic Peninsula by Ortega-Retuerta et al. (2010) (Table 6). Not only the high productivity but also very high level of CDOM in the ASP was confirmed. The ASP region appears to be enriched by biological production of CDOM from the relatively high productivity (Blough et al., 1993; Siegel et al., 2005).

The fate of the high CDOM in the euphotic layer in the ASP has three different the pathway: photobleaching, photohumification and biogeneration. If photobleaching is the one for fate of CDOM, the final product of bleaching will be CO_2, which will enhance the warming and ice loss in the ASP. If photohumification is the pathway after the light conditions is weaken in the late summer season, then the increase of POC with refractory OM will not significantly affect on the ice loss on the warming of seawater. However, if the biogeneration of CDOM by bacterial degradation in the major fate of the high CDOM, then the regeneration of CDOM can give smaller DOM or become of part of bacterial biomass (POC increase) or increase the non-photoreactive DOM pool.

Vertical distributions of CDOM appeared to be variable in the Amundsen Sea, with high CDOM at the surface to the subsurface layer. Maximal CDOM values at the surface were observed at the most of stations and maxima CDOM at the subsurface were observed at stations 2, 10, and 24 (Fig. 5). As reported by Ortega-Retuerta et al. (2010) in the Antarctic Peninsula, photobleaching of CDOM by UV radiation might reduce the concentration of CDOM at the surface. This profile reflects the combined effects of sunlight-

Table 6
Optical properties of CDOM and S values for different areas in the Southern Ocean.

Source of CDOM	$a_{CDOM}(\lambda)$ (m^{-1})		*S* value (μm^{-1})		Wavelength range (nm)	Reference
	average(λ)	range(λ)	average	range		
Crystal Sound	~0.25 (300)	–	23	–	260–330	Sarpal et al. (1995)
Paradise Harbor	~0.35 (300)	–	–	–		
Weddell Sea						
Seawater	–	0.01–0.78 (375)	–	11.1–39.6	300–650	Norman et al. (2011)
Bellingshausen Sea	0.41 (325)	–	17	12–19	275–295	Ortega-Retuerta et al. (2010)
Bransfield Strait	0.23 (325)	0.00–0.57	14	8–24		
Deception Island	1.30 (325)	0.73–2.17	18	17–19		
King George Island	0.18 (325)	0.00–0.26	29	24–39		
Amundsen Sea						
SIZ	0.14 (325)	0.11–0.17	18	12–26	275–295	**This Study**
ASP	1.07 (325)	0.49–2.01	20	11–39		
IS	0.40 (325)	0.36–0.43	31	11–28		

mediated bleaching of CDOM near the surface and the production of CDOM by phytoplankton at the subsurface (Carlson et al., 1994; Nelson et al., 1998). Interestingly, subsurface maximum of CDOM was observed at a few stations, which implied the extra source of CDOM in the water column. The subsurface high CDOM value exhibited at about 300–1000 m depth in our study area. We inferred that that MCDW could be an important source of fresh CDOM. MCDW flows into the Amundsen Sea over the sediment and through deep channels, the sediment is likely to be an important source of fresh DOM. Yager et al. (2012) reported that MCDW flows south from the shelf break and receives fresh DOM from sedimentary sources as interacts with the seabed through resuspension of sediment. Resuspended sedimentary fresh DOM may be mixed into the water column, resulting in the high CDOM at intermediate depths.

In our study, we observed higher a_{355} values in the water of high phytoplankton biomass (Fig. 6a) A significant positive correlation was observed between a_{355} and Chl-a within the euphotic layer ($r^2=0.70$, $n=30$, $p<0.05$) (Fig. 6a), variability in CDOM was dependent of Chl-a. Especially, CDOM was significantly related to the hex-fuco concentration ($r^2=0.78$, $n=30$, $p<0.05$) (Fig. 7b). Consequently, biological processes such as phytoplankton growth and bacterial degradation was proved as one of the main factors in the dynamics of CDOM in our study area. In particular, *P. antarctica* showed a key player in the biological process of CDOM production during austral summer in the Amundsen Sea. As Pavolv et al. (2013) reported, MAA is one of the important constituents of CDOM. Thus the high MAA concentrations from *Phaeocystis* sp. meant the higher CDOM production by *Phaeocystis* sp. compared to diatoms (*Thalassiosira* sp.). The study by Pavlov et al. (2013) was in agreement with our data, indicating the important contribution of *P. antarctica* to CDOM production.

Although $S_{300-500}$ values in our study area were not statistically different (ANOVA, $p<0.05$), the average value of $S_{300-500}$ was higher in the IS than in the SIZ and ASP (Table 5). Ortega-Retuerta et al. (2010) examined between salinity and $S_{275-295}$ in the Antarctic Peninsula in both January 2004 and February 2005. The $S_{275-295}$ is considered a good proxy for DOM molecular weight (Helms et al., 2008), indicating high value of $S_{275-295}$ means the nature of low molecular weight of DOM. To make comparison between S values form Ortega-Retuerta et al. (2010), we obtained the $S_{275-295}$ and CDOM at 325 nm (Table 6). The negative relationship between $S_{275-295}$ and salinity was encountered during 2005 (February), but no clear relationship was found in 2004. The authors explained that since sampling period in January 2004 was performed earlier than in 2005, lower values of Chl-a and bacterial abundance were observed, so the influences of ice melting were little pronounced in January 2004. Our sampling of CDOM was also performed in January 2014 and the effects of sea ice melting were small. No clear relationship between salinity and CDOM and the positive correlation between Chl-a and CDOM suggest that CDOM is likely associated with biological source with phytoplankton (*P. antarctica*) bloom in the ASP rather than ice melting in January 2014. The relatively high $S_{275-295}$ and a_{325} values in the ASP indicate the characteristic of young DOM with low molecular weight from the biological activity including photosynthetic production and grazing in the euphotic layer. The earlier opening of the ASP could extend the products season and enhance the magnitude of the phytoplankton bloom if enough light and Fe are available. In this event, the ASP could become a greatly carbon sink in the future. However, extending the open water season too much could reduce sea ice melt induced stratification and light limitation (Alderkamp et al., 2015) suggesting that carbon sink in the ASP also depends on the continued longevity of the surrounding seasonal marginal ice zone.

Compared to the previous study, our result of $S_{275-295}$ in the ASP was much higher than Bransfield strait and Bellingshausen Sea (Table 6). The high CDOM after the bloom could contribute to the absorption of light energy (heat absorption) and induce the increase of SSTs during summer season. The massive bloom of *P. antarctica* is known to make colony and the mucus of *P. antarctica* colony will produce high DOM. The *P. antarctica* bloom ends even before the light is still in good condition, that means the possibility of photobleaching and photohumification of CDOM in the euphotic zone till the end of summer.

5. Summary

In order to determine the phytoplankton taxonomy and CDOM variability, photosynthetic pigments, the absorption coefficient a_{355}, and the S values ($S_{300-500}$) were analyzed in the Amundsen Sea during austral summer in February 2012 and January 2014. In addition, environmental parameters such as salinity, SSTs, and nutrients were measured to determine the correlation between phytoplankton community composition and CDOM. Phytoplankton taxonomy in both summer of 2012 and 2014 was diverse with diatoms and *P. antarctica* as the major groups and cryptophytes, chlorophytes, cyanophytes, chrysophytes, and dinophytes as the minor groups.

Chl-a concentration in February 2012 (1.56 $\mu g\,L^{-1}$) was two-folds lower compared to Chl-a in January 2014 (2.40 $\mu g\,L^{-1}$), which showed peak in January, decreased rapidly at the end of summer. The CDOM values ranged from 0.07 to 0.98 m^{-1} and the average a_{355} was 0.51 m^{-1} in the ASP, 0.10 m^{-1} in SIZ and 0.16 m^{-1} in IS. In addition, when we recalculated the average of a_{CDOM} at 325 nm ranged from 0.14 to 1.07 m^{-1}, which was remarkably higher than any other CDOM values reported in the Southern Ocean. The variability of CDOM at three different regions and between the euphotic layer and below the ED was confirmed. In the Amundsen Sea, a positive correlation between CDOM and both Chl-a ($r^2=0.70$) and hex-fuco ($r^2=0.78$) and no clear correlation with salinity ($r^2=-0.01$) suggest that a biological source is the most important for the production of CDOM, especially from *P. antarctica*. Also it was demonstrated that relative contribution to the CDOM pool by *P. antarctica* was much higher than contribution by diatoms in the Amundsen Sea.

In future, progression of ice melting in the Amundsen Sea seems to continue to support the bloom of *P. antarctica* in the ASP regions, and in turn, CDOM in seawater is expected to increase. The longer opening period of polynya and the increased of ice-free areas also supports the duration of *P. antarctica* bloom. Moreover, this increased CDOM in the ASP and other polynya of the Southern Ocean could influence on the biogeochemical cycle of carbon, increased heat absorption, and photobleaching of CDOM at the surface of seawater Thus, our understanding of the fate of CDOM such as photobleaching, photohumification and biogeneration is critical to predict the acceleration of the ice melting and sequestration as feedback to increasing atmospheric CO_2 concentration.

Acknowledgments

We thank the captain and crew of the Korean IBRV Araon, for their outstanding assistance during the cruise. Our study supported by grants from Korea Polar Research Institute (KOPRI) (PP15020).

References

Amon, R.M.W., Benner, R., 1994. Rapid cycling of high-molecular-weight dissolved organic matter in the ocean. Nature 369 (6481), 549–552.

Alderkamp, A.C., Mills, M.M., van Dijken, G.L., Laan, P., Thuróczy, C.E., Gerringa, J.A., de Baar, J.W., Payne, C.D., Visser, J.W., Buma, G.J., Arrigo, K.R., 2012. Iron from melting glaciers fuels phytoplankton blooms in the Amundsen Sea (Southern Ocean): Phytoplankton characteristic and productivity. Deep-Sea Res. Part.II 71–76, 43–48.

Alderkamp, A.C., van Dijken, G.,L., Lowry, K.E., Connelly, T.L., Lagerström, M., Sherrell, R.M., Haskins, C., Rogalsky, E., Schofield, O.M., Stammerjohn, S.,E., Yager, P.L., Arrigo, K.R., 2015. Fe availability drives phytoplankton photosynthesis rates during spring bloom in the Amundsen Sea Polynya, Antarctica. Elem.: Sci. Anthr. 3 (1), 000043.

Arrigo, K.R., DiTullio, G.R., Dunbar, R.B., Robinson, D.H., van Woert, M., Worthen, D.L., Lizotte, M.P., 2000. Phytoplankton taxonomic variability in nutrient utilization and primary production in the Ross Sea. J. Geophys. Res. 105, 8827–8846.

Arrigo, K.R., van Dijken, G.L., 2003. Phytoplankton dynamics within 37 Antarctic coastal polynya systems. J. Geophys. Res. 108, C83271. http://dx.doi.org/10.1029/2002JC001739.

Arrigo, K.R., van Dijken, G.L., Bushinsky, S., 2008. Primary production in the Southern Ocean, 1997–2006. J. Geophys. Res. 113, C08004. http://dx.doi.org/10.1029/2007JC004551.

Barbini, R., Colao, F., Fantoni, R., Ferrari, G.M., Lai, A., Palucci, A., 2003. Application of a lidar fluorosensor system to the continuous and remote monitoring of the Southern Ocean and Antarctic Ross Sea: results collected during the XIII and XV Italian oceanographic campaigns. Int. J. Remote. Sens. 24 (16), 3191–3204.

Blough, N.V., Zafiriou, O.C., Bonilla, J., 1993. Optical absorption spectra of water from the Orinoco River outflow: terrestrial input of colored organic matter to the caribbean. J. Geophys. Res. 98, 2271–2278.

Bricaud, A., Morel, A., Prieur, L., 1981. Absorption by dissolved organic matter in the sea (yellow substance) in the UV and visible domains. Limnol. Oceanogr. 26, 43–53.

Buma, A.G.J., Bano, N., Veldhuis, M.J.W., Kraay, G.W., 1991. Comparison of the pigmentation of two strains of the prymnesiophyte *Phaeocystis* sp. Neth. J. Sea Res. 27, 173–182.

Buma, A.G.J., Gieskes, W.W.C., Thomesn, H.A., 1992. Abundance of Cryptophyceae and chlorophyll b containing organisms in the weddell scotia confluence area in the spring 1988. Polar Biol. 12, 43–52.

Carder, K.L., Steward, R.G., Harvey, G.R., Ortner., P.B., 1989. Marine humic and fulvic acids: their effects on remote sensing of chlorophyll. Limnol. Oceanogr. 34, 68–81.

Carlson, C.A., Ducklow, H.W., 1996. Growth of bacterioplankton and composition of dissolved organic carbon in the Sarggaso Sea. Aquat. Microb. Ecol. 10, 69–85.

Carlson, C.A., Ducklow, H.W., Michaels, A.F., 1994. Annual flux of dissolved organic carbon from the euphotic zone in the northwestern Sarggaso Sea. Nature 371, 405–408.

Ducklow, H.W., Wilson, S.E., Post, A.F., Stammerjohn, S.E., Erickson, M., Lee, S.H., Lowry, K.E., Sherrell, R.M., Yager, P.L., 2015. Particle flux on the continental shelf in the Amundsen Sea Polynya and Western Antarctic Peninsula. Elem. Sci. Anthr. 3 (1), 000046.

Everitt, R.P., Wright, S.W., Volkman, J.K., Thomas, D.P., Lindstrom, E.J., 1990. Phytoplankton community compositions in the western equatorial Pacific determined from chlorophyll and carotenoid pigment distributions. Deep-Sea Res. Part. A 30, 871–886.

Fragoso, G.M., Smith, W.O., 2012. Influence of hydrography on phytoplankton distribution in the Amundsen and Ross Seas, Antarctica. J. Mar. Syst. 89, 19–29.

Gordon, L., I., Jennings Jr, J., C., Ross, A., A., Krest, J., M., 1993. A Suggested Protocol for Continuous Flow Automated Analysis of Seawater Nutrients (Phosphate, Nitrate, Nitrite And Silicic Acid) in the WOCE Hydrographic Program and the Joint Global Ocean Fluxes Study. WOCE Hydrographic Program Office, Methods Manual WHPO 91-1.

Hahm, D.S., Rhee, T.S., Kim, H.C., Park, J.S., Kim, Y.N., Shin, H.C., Lee, S.H., 2014. Spatial and temporal variation of net community production and its regulating factors in the Amundsen Sea, Antarctica. J. Geophys. Res. Ocean. 119, 2815–2826. http://dx.doi.org/10.1002/2013JC009762.

Hansell, D.A., Carlson, C.A., 2002. Biogeochemistry of Marine Dissolved Organic Matter. Academic Press, San Diego.

Helms, J., Stubbins, R., Ritchie, A., Minor, J.D., Kieber, E.C., Mooper, K., D.J., 2008. Absorption spectral slopes and slope ratios as indicators of molecular weight, source, and photobleaching of chromophoric dissolved organic matter. Limnol. Oceanogr. 53, 955–969.

Hill, V.J., 2008. Impacts of chromophoric dissolved organic material on surface ocean heating in the Chukchi Sea. J. Geophys. Res. 113, C07024.

Jeffrey, S.W., Mantoura, R.F.C., Wright, S.W., 1997. Phytoplankton Pigments in Oceanography: Guidelines to Modern Methods. UNESCO Publishing, pp. 74–75.

Kieber, D.J., McDaniel, J., Mopper, K., 1989. Photochemical source of biological substrates in seawater: implication for carbon cycling. Nature. 341 (6243), 637–639.

Martin, J.H., Knauer, G.A., Karl, D.M., Broenkow, W.W., 1987. VERTEX: carbon cycling in the northeast pacific. Deep-Sea Res. Part. A 34 (2), 267–285.

Lee, S.H., Kim, B.K., Yun, M.S., Joo, H.T., Yang, E.J., Kim, Y.N., Shin, H.C., Lee, S.H., 2012. Spatial distribution of phytoplankton productivity in the Amundsen Sea, Antarctica. Polar Biol. . http://dx.doi.org/10.1007/s00300-012-1220-5

Nelson, N.B., Siegel, D.A., 2002. Chromophoric DOM in the open ocean. In: Hansell, D.A., Carlson, C.A. (Eds.), Biogeochemistry of Marine Dissolved Organic Matter. Academic Press, San Diego, pp. 509–546.

Nelson, N.B., Siegel, D.A., Michaels, A.F., 1998. Seasonal dynamics of colored dissolved organic matter in the Sargasso Sea. Deep-Sea Res. Part I 45, 931–957.

Norman, L., Thomas, D.N., Stedmon, C.A., Granskog, M.A., PASPadimitriou, S., KrASPp, R.H., Meiners, K.M., Lannuzel, D., van der Merwe, P., Dieckmann, G.S., 2011. The characteristics of dissolved organic matter and chromophoric dissolved organic matter in Antarctic sea ice. Deep-Sea Res. Part. II 58, 1075–1091.

Ortega-Retuerta, E., Reche, I., Villena, E.P., Agusti, S., Duarte, C.M., 2010. Distribution and photoreactivity of chromophoric dissolved organic matter in the Antarctic Peninsula. Mar. Chem. 118, 129–139.

Osburn, C.L., Retamal, L., Vincent, W.F., 2009. Photoreactivity of chromophoric dissolved organic matter transported by the Mackenzie River to the Beaufort Sea. Mar. Chem. 115, 10–20.

Park, M.G., 1999. New and regenerated production in the Yellow Sea: their environmental control and the estimation of new production by bio-optical methods (Ph. D. thesis). Seoul National University, p. 195.

Park, M.O., Park, J.S., 1997. HPLC method for the analysis of chlorophylls and carotenoids from marine phytoplankton. J. Oceanol. Soc. Korea 32, 46–55.

Pavlov, A.K., Silyakova, A., Granskog, M.A., Bellerby, R.G.J., Engel, A., Schulz, K.G., Brussaard, C.P.D., 2013. Marine CDOM accumulation during a coastal Arctic mesocosm experiment. J. Geophys. Res. Biogeosci. 119, 1216–1230.

Pegau, W.S., 2002. Inherent optical properties of the central Arctic surface waters. J. Geophys. Res. 107 (C10), 8035.

Priddle, J., Boyd, I.L., Whitehouse, M.J., Murphy, E.J., Croxall, J.P., 1998. Estimates of Southern Ocean primary production-constraints from predator carbon demand and nutrient drawdown. J. Mar. Syst. 17, 275–288.

Rignot, E., 2001. Evidence for rapid retreat and mass loss of Thwaites Glacier, West Antarctica. J. Glaciol. 47, 213–222.

Sarpal, R.S., Mopper, K., Kieber, D.J., 1995. Absorbance properties of dissolved organic matter in Antarct Seawater. Antarct. J. US 30, 139–140.

Shadwick, E.H., Rintoul, S.R., Tilbrook, B., Williams, G.D., Young, N., Fraser, A.D., Marchant, H., Smith, J., Tamura, T., 2013. Glacier tongue calving reduced dense water formation and enhanced carbon uptake. Geophys. Res. Lett. 29, 7. http://dx.doi.org/10.1029/2001GL014160.

Siegel, D.A., Maritorena, S., Nelson, N.B., Behernfeld, M.J., 2005. Independence and interdependencies of global ocean color properties: reassessing the bio-optical assumption. J. Geophys. Res. 110, C07011. http://dx.doi.org/10.1029/2004JC002527.

Smith Jr., W.O., Dinniman, M.S., Tozzi, S., DiTullio, G.R., Mangoni, O., Modigh, M., Saggiomo, V., 2010. Phytoplankton photosynthetic pigments in the Ross Sea: patterns and relationships among functional groups. J. Mar. Syst. 82, 177–185.

Stedmon, C.A., Amon, R.M.W., Rinehart, A.J., Walker, S.A., 2011. The supply and characteristics of colored organic matter (CDOM) in the Arctic Ocean: Pan Arctic trends and differences. Mar. Chem. 124, 108–118.

Takahashi, T., Sutherland, S.C., Wanninkhof, R., Sweeney, C., Feely, R.A., Chipman, D.W., Hales, B., Friederich, G., Chavez, F., Sabine, C., Watson, A., Baker, D.C.E., Schuster, U., Metzl, N., Yoshikawa-Inoue, H., Ishii, M., Midorikawa, T., Nojiri, Y., Körtzinger, A., Steinhoff, T., Hoppema, M., Olafsson, J., Amarson, T.S., Tilbrook, B., Johannessen, T., Olsen, A., Bellerby, R., Wong, C.S., Delile, B., Bates, N.R., de Baar, H.J.W., 2009. Climatological mean and decadal change in surface pCO_2 and net sea-air CO_2 flux over the global ocean. Deep-Sea Res. Part. II 56, 554–577.

Tyler, J.E., 1975. The in situ quantum efficiency of natural phytoplankton populations. Limnol. Oceanogr. 20, 976–980.

Yager, P.L., Sherrell., R.M., Stammerjohn, S.E., Alderkamp, A.C., Schofield, O., Abrahamsen, E.P., Arrigo, K.R., Bertuksson, S., Garay, D.L., Guerrero, R., Lowry, K.E., Moksnes, P.O., Ndungu, K., Post, A.F., Randall-Goodwin, E., Riemann, L., Severmann, S., Thatje, S., van Dijken, G.L., Wilson, S., 2012. ASPIRE: the Amundsen Sea Polynya international research expedition. Oceanography 25 (3), 40–53.

Yager, P.L., Wallace, D.W.R., Johnson, K.M., Smith Jr, W.O., Minnett, P.J., Deming, J.W., 1995. The northeast water Polynya as an atmospheric CO_2 sink: a seasonal rectification hypothesis. J. Geophys. Res. 100, 4389–4398.

Yang, E.J., Kim, S.Y., Lee, S.H., 2013. Trophic role of microzooplankton in *Phaeocystis* and diatom dominated waters in the Amundsen Sea. Antarctica.

Weber, T.S., Deutsch, C., 2010. Ocean nutrient ratios governed by plankton biogeography. Nature 467, 550–554.

Zepp, R.G., Erickson, D.J., Pual, N.D., Sulzberger, b, 2007. Interactive effects of solar UV radiation and climate change on biogeochemical cycling. Photochem. Photobiol. Sci. 6, 286–300. http://dx.doi.org/10.1039/b700021a.